JOURNAL OF NANO- AND ELECTRONIC PHYSICS
Vol. 10 No 5, 05021(6pp) (2018)

ЖУРНАЛ НАНО- ТА ЕЛЕКТРОННОЇ ФІЗИКИ
Том 10 № 5, 05021(6cc) (2018)

Nano Silicon Carbide's Stacking Faults, Deep Level's and Grain Boundary's Defects

S.I. Vlaskina[1], G.S. Svechnikov[2], G.N. Mishinova[3], V.I. Vlaskin[4], V.E. Rodionov[5], V.V. Lytvynenko[6]

[1] *Yeoju Institute of Technology (Yeoju University), 338, Sejong-ro, Yeoju-eup, Yeoju-gun, Gyeonggi-do, 469-705 Korea,*

[2] *National Technical University of Ukraine "Igor Sikorsky Kyiv Polytechnic Institute", 37, Peremohy Ave., Kyiv, Ukraine,*

[3] *Taras Shevchenko Kyiv National University, 64, Volodymyrs'ka Str., 01033 Kyiv, Ukraine*

[4] *H&P Corp. Techno 2-ro, 119 Yongsan-dong 516-1, 34024 Daejeon, Korea*

[5] *State Institution "Institute of Environmental Geochemistry, NAS of Ukraine", 34A, Academician Palladin Ave., Kyiv, Ukraine*

[6] *Institute of Electrophysics and Radiation Technologies NAS of Ukraine, p.o. box. 8812, 28, Chernyshevskiy Str., 61002 Kharkiv, Ukraine*

(Received 05 September 2018; revised manuscript received 22 October 2018; published online 29 October 2018)

In this work, photoluminescence spectra of SiC crystals with ingrown original defects are analised It was shown that stalking fault and deep level luminescence spectra reflect the fundamental logic of the SiC polytype structure .The analysis of the zero- phonon spectra of the stalking fault, deep level, and grain boundary parts of the photoluminescence spectra makes it possible to control the processes of phase transformations within the growth process of crystals and films, as well as during the technological operations. Moreover, it makes it possible in nanostructures of silicon carbide. to determine the position or displacement of atoms participating in the photoluminescence with an accuracy of 0.0787 Angstrom (or 1.075 meV)

Keywords: Silicon carbide, Polytype, Stacking fault, Photoluminescence spectra.

DOI: 10.21272/jnep.10(5).05021 PACS numbers: 78.20. – e, 78,55.m, 78.67.Bf

1. INTRODUCTION

Silicon carbide (SiC), films and Nano-silicon carbide are a semiconductor with a lot of fundamental optical properties of crystals (polytypes) and nanocrystals (nanopolitips). Silicon carbide exists as several different polytypes according to the stacking sequence of SiC atomic double layers in the crystal lattice. Great advances were reported in growing a single crystalline polytype by controlled sublimation and chemical vapor deposition.

Silicon carbide is an example of wide band gap semiconductors with chemical, electrical and optical properties that make them very attractive for applications under extreme conditions. Their unique electrophysical properties make it possible to use them as detectors of ionizing radiation, along with other semiconductors [1], high radiation-thermal resistance allows using them in radiation technologies [2] and also as protective coatings for active zone materials [3] of nuclear reactors.

Polytypic transformation in SiC was investigated by many authors [4-12] Extremely chemically inert solid SiC is the candidate for the next-generation optoelectronics: devices with high power, frequency and temperature operation [13]. While there are over 170 known polytypes of SiC, only a few are commonly grown in a reproducible form acceptable for use as an electronic semiconductor. The most common polytypes of SiC presently being developed for electronics are the cubic 3C-SiC, the hexagonal (α) 4H-SiC and 6H-SiC. The determination of cubic or hexagonal structures in crystals has shown that the optical properties of different polytypes strongly depend on the defects[14].

For the nanocrystals with the dimensions below 1 nm, only one crystal structure can exist. The nanocrystals with large diameters (1-3 nm and more) can be represented by cubic and hexagonal polytypes.

Photoluminescence of the SiC nanocrystals was discussed in [15]. It was shown that the photoluminescence spectrum is very structured. The small slit width (equal to 0.5 meV) for the low-temperature spectroscopic studies makes it possible to detail the spectra and reveal their fine structure and to monitor the phase transformation processes by determine the position or mixing of atoms participating in the photoluminescence within 0.0787 Angstrom (1.075 meV).

The aim of this work is further investigation and structures of the temperature-dependent luminescence spectra in SiC crystals, films and nanocrystals.

2. EXPERIMENT

The method of optical spectroscopy low temperature photoluminescence(LTPL) was used in this work, as it is reveals high sensitivity to the structural changes.

In the PL experiments, nitrogen LGI-21 operating at the wavelength 337 nm (3.68 eV), helium-cadmium LG-70 – 441.6 nm (2.807 eV) and Ar+-lasers $\lambda = 488$ nm, $h\nu = 2.54$ eV, respectively, were used. Also, mercury ultrahigh pressure lamp SVDSh-1000 with the UV-2 filter, and xenon lamp DKSSh-1000 were used.

The PL spectra were measured using the samples contained in a liquid helium or nitrogen cryostat, which provided temperatures ranging from 1.5 to 330 K.

PL spectra of lightly doped SiC single crystals and films with the impurity concentration of ND – NA ~ (2-8)$\cdot 10^{16}$ cm^{-3}, ND ~ (5-8)$\cdot 10^{17}$ cm^{-3}, and ND–NA > 3$\cdot 10^{17}$ cm^{-3}, ND ≥ 1$\cdot 10^{18}$ cm^{-3} (NDL-samples) were investigated.

The analysis of absorption, excitation and low tem-

© 2018 Sumy State University

perature photoluminescence spectra suggests formation of a new micro-phase during the growth process and appearance of the deep-level (DL) spectra.The stalking fault spectra (SF)indicate the metastable formation of nano-structures in the SiC crystals.

The PL spectra in SiC single crystals and films were investigated within the temperature range 4.2 to 77 K.

The α-SiC crystals under consideration were divided in three groups: pure SiC crystals and films with non-compensated concentration ND – NA ~ (4-9) ~ 10^{16} cm^{-3}, NA ~ (1-3)·10^{16} cm^{-3}; b) lightly doped samples with ND – NA ~ (2-8)·10^{16} cm^{-3}, ND ~ (2…7)·10^{17} cm^{-3}; c) doped samples with ND – NA > 3·10^{17} cm^{-3}, ND > ~ 1·10^{19} cm^{-3}.

Dependence of intensity of the DLi spectra on impurity concentration is shown in Fig. 1, where shaded area – the SFi spectra from ref.[17], (a) - most pure samples with only SF spectra, ND – NA ~ (4-9) ~10^{16} cm^{-3}, NA ~ (1-3)·10^{16} cm^{-3}; ND – NA ~ (4-9) 10^{16} cm^{-3} (1-5) 10^{16} cm^{-3}, ND < 1 10^{17} cm^{-3}, NA < (1-3) 10^{16} cm^{-3} from ref. [19], (b) – pure samples with the SFi and DLi series ND – NA ~ (2-8)·10^{16} cm^{-3}, ND ~ (2-7)·10^{17} cm^{-3}; (c) – doped samples with ND – NA > 3·10^{17} cm^{-3}, ND > ~ 1·10^{19} cm^{-3}.

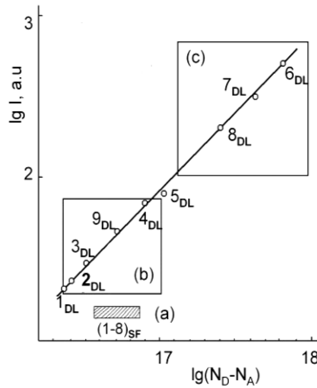

Fig. 1 - Intensity of DLi spectra (i = 1) (T = 77 K) at 2.4-2.5 eV vs impurity concentration for different samples (the SFi and DLi series)

3. RESULTS AND DISCUSSIONS

Low-temperature photoluminescence spectra of SiC and the structure of zero phonon parts of the deep level (DL) spectra [16], stacking fault (SF) [17] and grain boundary (GB) are shown in Fig. 2.

The phonons of the extended Brillouin central zone (LO 119-120 meV) and the local phonon (LOC 91 meV) participates in the structure of the DL1 spectra. The fine structure of the zero-phonon part of the spectrum is divided into two groups (DL-I or DL-X and DL-II or DL-Y). which have the same energy width and two parts superimposed on each other. The position of the center of symmetry in the zero-phonon parts is located in the center of their superposition.

The energy width of the zero phonon part of the SF spectrum is calculated to be the same as the energy width for each part of the DL spectrum. The remaining part of the spectrum is described by including phonon replicas of the edges of the Brillouin zone TA-46, LA-77, TO-95 and LO-104 (Fig. 2 c)

The analysis of the zero-phonon part of SF1 spectrum shows that the SF spectrum also consists of two components: SF-I and SF-II and its structure repeats the structure of the DL spectrum. Two parts of the zero-phonon SF spectrum overlap. The position of the center of symmetry in the zero-phonon parts is located in the center of the overlap region.

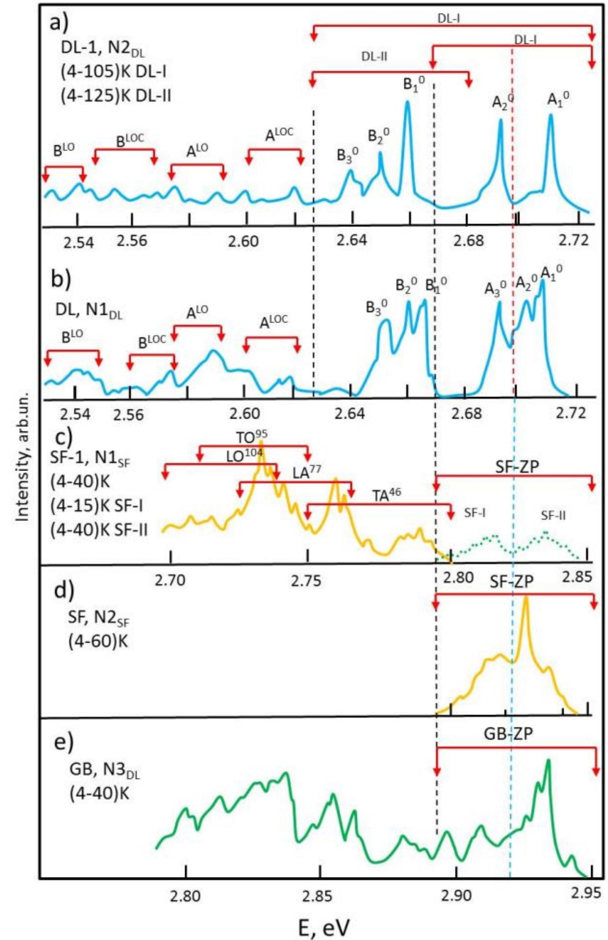

Fig. 2 - Low-temperature spectra of photoluminescence and the structure of zero phonon parts of the Deep Level (DL, Stacking Fault (SF) and Grain Boundary (GB)) spectra for different samples of sample N1DL with ND – NA is 2·10^{16} cm^{-3}, the sample of N2DL with ND-NA is 3·10^{16} cm^{-3}

The zero-phonon part of SF spectrum after plastic deformation is shown in Fig. 2 d.

The energy width of the zero phonon part of the GB spectrum coincides with the energy width of each part of DL spectrum and is equal to the energy width of the zero phonon part of the SF spectrum. The GB spectrum is shown when interacting with edge phonons TA-46, LA-77, TO-95, LO-104 at temperatures (4.2-40 K). But, unlike the SF spectra, the presence of the zero-phonon part here (in GB) is in the obvious manifestation (Fig. 2 e.).

The SFi and GB spectra and the corresponding spectra of photo-luminescence excitation at T = 4.6 K are shown in Fig. 3 The long-wave front of the excitation spectra for the DLi and SFi spectra is the same (i = 1 → E_{gx} (14H1), i = 2 → E_{gx} (10H2), i = 3 → E_{gx} (14H2) The arrows (↓, ↑) indicate the PL spectra, for

which excitation spectra were recorded.

The behavior of the fine structure of zero-phonon SF, DL, and GB spectra is presented in Table 1. Various recording conditions and various effects on crystals and SiC films were used. Table 1 is a summary of all previous studies of SF, DL and GB spectra.

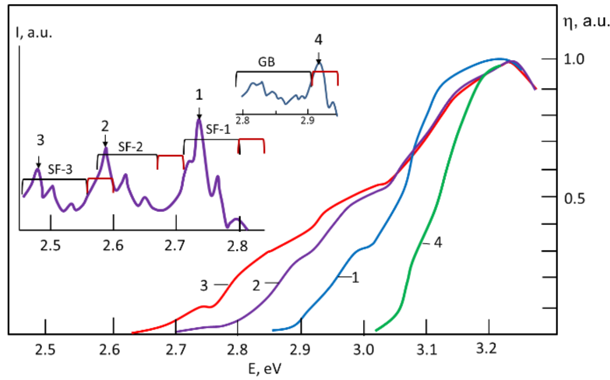

Fig. 3 - SFi, GB spectra and corresponding photoluminescence excitation spectra at $T = 4.6$ K for sample N5SF with ND – NA = 4·10¹⁶ cm⁻³, ND < 1·10¹⁷ cm⁻³, NA ~ 3·10¹⁶ cm⁻³

Thus, a detailed study of the spectra of low-temperature luminescence in SiC crystals showed that, starting from the energy position of the SFi spectra, the DLi spectra, and the GB spectra, the nano- and microstructure of the ordered regions consists of thin lamellae (10-100 A), which are a set of twin wafers □ -phase and such basic α -SiC structures as

15R <23> (a = 12.5 A),
6H <33> (a = 15 A),
15R <23> (a = 12.5 A),
21R <34> (a = 17.5 A),
8H <44> (a = 20 A),
10H <55> (a = 25 A) and
14H <77> (a = 35 A).

In this case, the degree of one-dimensional disordering is also fixed by diffusion of diffraction reflections on he Laue pattern SFi and DLi spectra seem to follow the structural rearrangement. Fig. 4, 5 shows the zero-phonon parts of the SF, DL and GB spectra in SiC. Spectra in Si and CdS are also given for comparison and analysis [18]. The SF and DL spectra consist of two parts superimposed on each other. In this case, the width (in the energy scale) of the SF spectrum is equal

Table 1 - The behavior of the fine structure of zero-phonon SF, DL, and GB spectra under various recording conditions and various effects on crystals and SiC films

Type of spectrum / Nature of manifestation		**Staking faults (SF)**	**Deep Lever (DL)**	**Grain Boundary (GB)**
Degree of structural disorder in initial grown crystal	д-I	SF-1	DL-1	Some time is absorbed
	д-II	∑SFi (i = 1,2…6)	∑DLi	Some time is absorbed
Impurity concentration	(a)	Dominate	As background of SF	Fine structure is weakly absorbed
	(b)	Possibly (weakness)	A fine structure appears	The fine structure is clearly absorbed
	(c)	Absent	Blurring the fine structure	Not absorbed
	Note	SF (weakness) are also observed at ND – NA ~ (7-8)·10¹⁷ cm⁻³ if acceptor concentration low as NA ~ (1-3)·10¹⁶ cm⁻³	At 77 K (a) – 0.1I Intensity (b) – I Intensity (c) – 10I Intensity	N/A
Possible combinations of this type of spectrum with others		With DL – genetic link With GB – usual exist	N/A	Is absorbed together SF and DL for (a) and (b); for (c) not absorbed
Structure of the spectrum	Non-phonon (eV)	SF-1 (2.853-2.793) SFI (2.853-2.819) SFII (2.827-2.793)	DL-1 X(2.73-2.67) Y(2.685ч2.625) Fine structure	2.95-2.89, the fine structure is clearly absorbed for (b)
	Interaction with phonons (meV)	Phonons of the edge of the extended Brillouin zone of SiC (TA-46, LA-77, TO-95, LO-104) were involved	LOC-91 LO-120	TA-46 LA-77 TO-95 LO-104

Dependence of luminescence spectra from	Temperature of samples (K)	Range of observa-tion (Ko)	SF-1 (4.2-35) SFI (4.2-15) SFII (4.2- 35)	X(4.2-105), Y(4.2-125) Background till 160-170	4.2-40
		Behavior of the fine stricture elements	Differential change luminescent intensity of fine structure ДН = 1.5-2 meV, at 4.2 K	Increasing intensity of fine structure at (4.2-30), LOC disappear at 30 K, the broadening of the fine structure is proportional kT with short wavelength shift $T > 60$ K, X attenuation fester then Y	Synchronous temperature attenuation of all fine structures
		Thermal energy of extinguishing	SFI – 3.5 meV SFII – 7 meV	$E_a(X) = 0.21 \pm 0.01$ eV $E_a(Y) = 0.26$ eV at $T = 660$ K	$E_a = 7$ meV
Intensity and Energy of exiting light			$I_{lum} = I^{б}_{exciting}$ ($б = 0.7 \pm 0.1$) relative intensity luminescent doesn't change, $I_{lum} = 0.05$ $I_{exiting}$ at $I_{exiting} = 0.005$ I_0	$I_{lum} = I^{б}_{exciting}$ ($б = 0.7$-0.9), short wavelength of spectrum decrease fester	$I_{lum} = I^{б}_{exciting}$ ($б = 0.7$) short of spectrum decrease fester
Character attenuation of spectrum luminescent at different delay time			$I_{lum} = 0.02 \cdot I_0$ at $t = 3$ ms (4.2 K). SFI is faster attenuation	$I_{lum} = I_0 \cdot t^{-б}$, $t = 0.1$ µs-10 ms, at $T = 4.2$ K $б_1 = 1.5$, $б_2 = 0.4$, at $T = 77$ K, $б = (0.7$-$0.9)$	$I_{lum} = I_0 \cdot t^{-б}$ at $t = 3$-15 ms, short wavelength of spectrum decrease fester
Polarization of exciting light			At Eexciting II c intensity of SFII is decreased	Differential change luminescent intensity of fine structure X, Y (4.2 K)	At Eexciting II c intensity of SFII is decreased
Plastic deformation			SF-1 appearances	DL appearances in pure sample SiC, in crystal lightly doped DL increases	GB appearances in pure sample SiC
High Temperature annealing			SF-1 appearances in β-SiC, short wavelength of spectrum decreases in б-SiC	Fine structure without change, background increases in doped crystals	GB appearances in β-SiC

to the width of the GB spectrum and is equal to the width of each of the parts of the DL spectrum.

Thus, DL and SF spectra hand-in-hand follow the structure transformations. Same as the SF, the DL spectra comprise two parts superposing each other. Here, the energy width of the SF spectrum equals the width of each part of the DL spectrum. If one could draw a line through the middle of superposing parts DL-X, DL-Y and SF-I, SF-II and estimate E_g for the different polytypes (Table 2) the intelligible correlation is revealed (Tables 3, 4). From the data above, the DL luminescence spectra reflect the fundamental logic of SiC polytype structure. Owing to it, one can observe the structure changes caused by the phase transformations and growth of SiC polytypes and their aggregates.

From the comparison of the difference between the position of the center of symmetry of the zero-phonon part of the SF (correlated with E_{gx}) and the position of the center of symmetry DL (X) with the difference between the position of the center of symmetry of the zero-phonon part of the SF (correlated with Egx) and the position of the center of symmetry DL(Y) It can be seen that the experimentally obtained shift (shift between the centers $\Delta 1$-$\Delta 2 = 0.043$ eV) is just a half the value of 0.086 eV [17].

Thus, the photo luminescence spectra of SF DL, and GB reflect the fundamental laws governing the structure of SiC polytypes. If the Si spectrum is applied to the spectrum of β-SiC DL (there are no binaryities in silicon, therefore, only 2 spikes), and correlated with the position of Si atoms and C atoms (Fig. 6) in the (1120)plane then to compare the values of the width of the zero-phonon line DL, it is clear that the entire picture of the DL, SF, and GB spectra is played out within three heights "h" in Fig. 6. It follows that, to within accuracy of 1/4i (0.0787 Angstrom or 1.075 meV) It is possible to monitor the structure (position of the atoms) from the zero-phonon spectra of SF, DL, and GB spectra.

The fine-structure elements of the zero-phonon part of the DL, SF, and GB spectra are a reflection of the interaction of specific silicon Si and carbon C atoms within four Si atoms formation(ABCA positions). Analysis of the spectra makes it possible to fix the interaction between both silicon atoms and between silicon and carbon atoms. This allows us to monitor the rearrangement of the structure during phase transformations and various

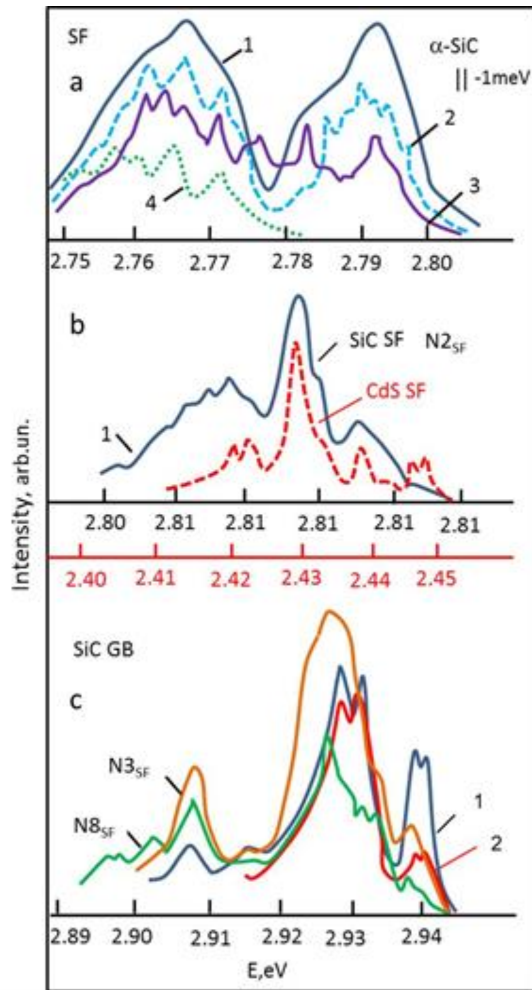

Fig. 4 - Zero-phonon parts of SF and GB spectra. a) - Zero-phonon parts of the SF spectra in SiC, calculated by the translation of the TA phonon. b) - Zero-phonon parts of the SF spectra in SiC and in CdS [18], actually manifested c) Zero-phonon parts in the GB spectra actually manifested: a-1- PL Spectrum of beta-SiC crystal in the phase transformation region of 3C-6H after a temperature-induced thermal shock; 2,3,4 – PL Spectra of defective packages, due to the growth process of SiC, sample $N5_{SF}$,$N8_{SF}$ and $N10_{DL}$ respectively; c-1,2 - sample $N2_{SF}$ before and after plastic deformation

Table 2 - Band gap (optical E_g and exitone E_{gx}) in SiC

Polytype	E_g	E_{gx}	$\Delta = E_g - E_{gx}$
6H	3.109	3.024	0.085
3R	3.087	3.002	0.085
21R	2.938	2.853	0.085
8H	2.868	2.783	0.085
10H2	2.798	2.713	0.085
14H2	2.698	2.613	0.085

Table 3 – Difference between the position of the centre of symmetry of the zero-phonon part of SF spectra(normalized to Egx) and the position of the centre of symmetry of DL-I (X) (data from Ref. [17])

Polytype	$SF^{Egx} – DL – I(X) = \Delta_1$
21R	2.823 – 2.698 = 0.125
$10H_2$	2.683 – 2.558 = 0.125
$14H_2$	2,583 – 2,458 = 0,125

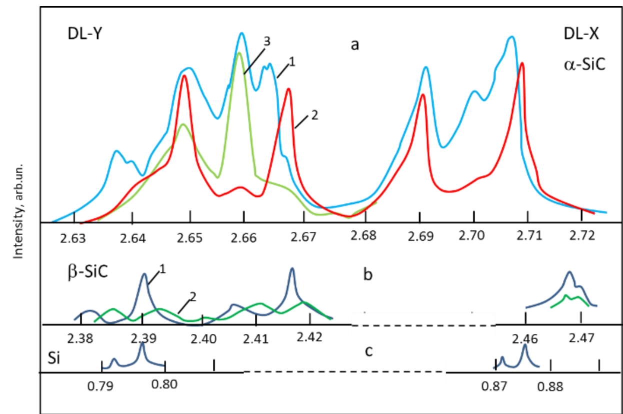

Fig. 5 – Zerro-phono parts of the DL spectra in SiC and Si: a – 1-$N1_{DL}$, 2- $N2_{DL}$, 3-$N6_{DL}$; b – 1- .$N2_{\beta}$, as grown joint polytypes 2-$N9_{\beta}$ in the zone of maximum deformation by bending at T = 2100 °C during 30 min, c – Si sample

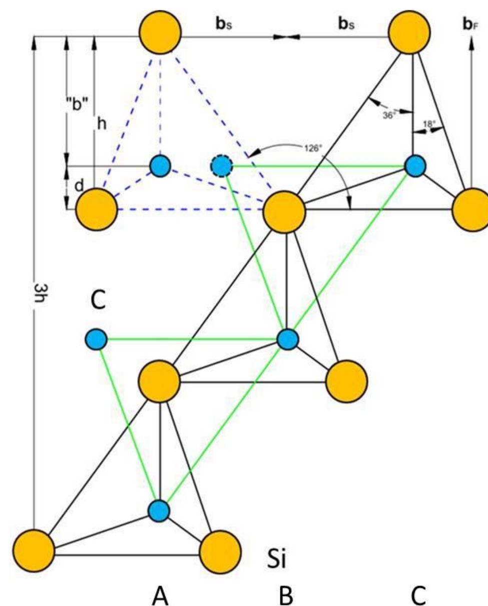

Fig. 6 – Lattice structure of cubic SiC

Table 4 – Difference between the position of the centre of symmetry of the zero-phonon part of SF spectra(normalized to Egx) and the position of the centre of symmetry of DL-II (Y) (data from Ref. [17])

Polytype	$SF^{Egx} – DL – II(Y) = \Delta_2$
21R	2.823 – 2.655 = 0.168
10H2	2.683 – 2.515 = 0.168
14H2	2.583 – 2.415 = 0.168

and various deviations in the positions of atoms of different polytypes and intergrowths of SiC polytypes.

4. CONCLUSION

It has shown that the spectra of DL and SF follow the structural transformations in SiC. The line through the middle of the superposed parts of DL-X, DL-Y and SF-I, SF-II spectra and the estimated Eg for different polytypes reveals a clear correlation. From the above data, SF and DL luminescence spectra reflect the fun-

damental logic of the structure of the SiC polytype.

Analysis of the spectra of the zero-phonon parts of SF, DL, GB spectra makes it possible to control the processes of phase transformations both with the growth of crystals and films, and in technological operations. Moreover, it is possible to determine the position or displacement of atoms participating in the PL with an accuracy of 0.0787 Angstrom or 1.075 meV in nanostructures of silicon carbide.

Дефекти упаковки наноструктурованого карбіду кремнію, дефекти глибоких рівнів та границь зерен

С.І. Власкіна[1], Г.С. Свєчніков[2], Г.М. Мішинова[3], В.І. Власкін[4], В.Є. Родіонов[5], В.В. Литвиненко[6]

[1] *Технологічний інститут Йою (Університет Йою), 338, Сейон-ро, Еою-ган, Гіеонжі-до, 469-705 Південна Корея*

[2] *Наіиональный технічний університет «Київський політехнічний інститут імені Ігоря Сікорського», пр. Перемоги, 37, Київ, Україна,*

[3] *Київський національний університет імені Траса Шевченка, вул.Володимирська, 64, 01033, Київ, Україна*

[4] *Корпорация Техно 2, 119 Йонгсан-донг 516-1, Дайджеон, Південна Корея, 34024*

[5] *Державна установа «Інститут геохімії навколишнього середовища НАН України», пр. Академіка Палладіна,34 А, 03680 Київ, Україна,*

[6] *Інститут електрофізики і радіаційних технологій НАН України, Чернишевського, 28, а/с 8812, 61002 Харків, Україна*

У роботі аналізуються фотолюмінесцентні спектри кристалів SiC з дефектами, що виникають при вирощуванні. Показано, що дефекти упаковки та глибокі рівні люмінесцентного спектру відображають закономірності політичної структури SiC .Аналіз спектру нульових фотонів дефектів упаковки, глибоких рівнів і ганиць зерен в фотолюмінесцентному спектрі дає можливість контролювати процеси фазових перетворень при вирощуванні кристалів та плівок а також при проведенні технологічних операцій. Більш того, це також дає можливість в наноструктурованому карбіді кремнію визначати положення або зсув атомів, що беруть участь в фотолюмінесценції з точністю до 0,0787 ангстрем (або 1,075 меВ)

Ключові слова: Карбід кремнію, Політип, Дефект упаковки, Спектр фотолюмінесценції.

REFERENCES

1. A.A. Zaharchenko, A.I. Skrypnyk, M.A. Khazhmuradov, E.M. Prohorenko, V.F. Klepikov, V.V. Lytvynenko, *Probl. Atom. Sci. Tech.* **85** No 3, 231 (2013).
2. V.T. Uvarov, V.V. Uvarov, V.N. Robuk, N.I. Bazaleev, A.G. Ponomarev, A.N. Nikitin, Yu.F. Lonin, T.I. Ivankina, V.F. Klepikov, V.V. Lytvynenko, S.Ye. Donets, *Phys. Part. Nucl. Latter.* **11**, No 3, 274 (2014).
3. V.F. Klepikov, Yu.F. Lonin, V.V. Lytvynenko, A.G. Ponomarev, O.S. Startsev, V.T. Uvarov, *J. Nano-Electron. Phys.* **7** No 4, 04016 (2015).
4. P. Pirouz, M. Zhang, H.McD. Hobgood, M. Lancin, J. Douin, and B. Pichaud, *Phil. Mag. A* **86**, 4685 (2006).
5. I.S. Gorban, G.N. Mishinova, *Proc. SPIE* **3359**, 187 (1998).
6. A. Galeckas, H.K. Nielsen, J. Linnros, A. Hallén, B.G. Svensson, and P. Pirouz, *Mater. Sci. Forum* **483**, 327 (2005).
7. S.I. Maximenko, T. Sudarshan, P. Pirouz, *Appl. Phys. Lett.* **87**, 033503 (2005).
8. A. Galeckas, J. Linnros, P. Pirouz, *Phys. Rev. Lett.* **96**, 025502 (2006).
9. S.I. Maximenko, P. Pirouz, T.S. Sudarshan, *Mater. Res. Forum* **527-529**, 439 (2006).
10. H. Idrissi, B. Pichaud, G. Regula, M. Lancin, *J. Appl. Phys.* **101**, 113533 (2007).
11. G.R. Fisher, P. Barnes, *Phil. Mag., Part B* **61**, 217 (1990).
12. Sh. Sugiyama, M. Togaya *J. Am. Cer. Soc.* **84**, 3013 (2001).
13. S. Askari, A. Hag, M.l Macias-Montero, I. Levchenko, F. Yu, W. Zhou, K. Ostrikov, P.l Maguire, V. Svrcek, D. Mariotti, *Nanoscale* **8**, 17141 (2016).
14. S.I. Vlaskina, S.P. Kruchinin, E.Ya. Kuznetsova, V.E. Rodionov, G.N. Mishinova, G.S. Svechnikov, *Int. J. Mod. Phys. B* **30**, 13 (2016).
15. D. Beke, Z. Szekrényes, Z. Czigány, K. Kamarás Á. Gali, *Nanoscale* **7**, 10982 (2015).
16. S.I. Vlaskina, G.N. Mishinova, V.I. Vlaskin, V.E. Rodionov, G.S. Svechnikov. *Semicond. Phys., Quantum Electron. Optoelectron.* **16** No 3, 272 (2013).
17. S.I. Vlaskina, G.N. Mishinova, V.I. Vlaskin, G.S. Svechnikov, V.E. Rodionov *Semicond. Phys., Quantum Electron. Optoelectron.* **18** No 2, 209 (2015).
18. Yu.A. Osipyan, V.D. Negryi *phys. stat. sol (a)* **55**, 583 (1979).